Materials Science Forum Vols. 331-337 (2000) pp. 1473-1478

Numerical Modelling of Roughness and Plasticity Induced Crack Closure Effects in Fatigue

M.R. Parry[1], S. Syngellakis[2] and I. Sinclair[1]

[1] Materials Research Group, University of Southampton, School of Engineering Sciences, Highfield, Southampton, SO17 1BJ, UK

[2] Computational Engineering and Design Groups, University of Southampton, School of Engineering Sciences, Highfield, Southampton, SO17 1BJ, UK

Keywords: Crack Closure, Elastic-Plastic Finite Element Analysis, Fatigue Crack Growth, Slip Behaviour

Abstract. The incidence of roughness induced fatigue crack closure has been studied by finite element modelling. Based on an analysis of both overall specimen compliance and node behaviour along the crack path the present modelling shows: (a) an increasing effect of crack path angle on roughness induced closure levels in keeping with the simple analytical model of Suresh and Ritchie; (b) the mechanism by which closure occurs is due to residual plastic strains in the wake, rather than global shear displacements of the fracture surfaces due to mixed-mode behaviour at the crack tip; and (c) the closure levels are relatively low compared to experimental data, consistent with the absence of environmental irreversibility in the finite element models and the idealised crack path morphologies that were used. Slip band simulations show a significant increasing effect of inhomogeneous deformation on closure levels, improving the apparent accuracy of the modelling results.

Introduction

The phenomenon of fatigue crack closure is widely considered to have a strong influence on fatigue crack growth. Many aluminium aerospace alloys exhibit microscopically deflected crack growth modes, and various aspects of fatigue crack growth have been rationalised by the associated incidence of roughness induced crack closure (RICC) [1]. An extensive body of experimental evidence and theoretical analysis has developed to support the dependence of fatigue crack growth on closure phenomena. Several quantitative and semi-quantitative models of RICC exist within the literature, although they are generally rather simplified. Furthermore, interactions between different closure mechanisms are largely ignored. The present work seeks to extend current quantitative understanding of RICC, focusing on geometrical and micromechanical closure effects, for a propagating elastic-plastic crack.

Background. Elber [2] noted that as a fatigue crack propagates, plastically stretched material in the crack wake leads to premature contact of the crack faces, a process referred to as plasticity induced crack closure (PICC). Other mechanisms by which shielding of the crack tip can occur have been identified (e.g. see [3]). The possibility that crack path roughness may lead to premature crack closure was first reported by Walker and Beevers [4], who studied fatigue crack growth in titanium samples and found that whilst PICC effects were apparently absent, contact occurred at discrete points behind the crack tip as a result of deflected crack growth and the associated shear of the crack flanks. In order for RICC to occur a combination of crack path deflection and a residual shear offset of the fracture surfaces is clearly required. At the tip of a deflected crack mixed mode loading conditions will exist, which may then lead to a global shear offset of the fracture surfaces due to irreversibility of the local plastic deformation.

Modelling of closure. Newman and Armen [5] used the finite element method to model PICC. Using an essentially arbitrary crack growth algorithm and continuum plasticity theory, a model of a cracked plate was constructed. It was predicted that the crack faces come into contact under tensile

far field loads in agreement with experimental observations. Several attempts have been made to model RICC effects. Suresh and Ritchie [6] derived an expression for the closure stress intensity factor for RICC using a simple geometrical model of a deflecting crack,

$$\frac{K_{cl}}{K_{max}} = \sqrt{\frac{\chi \tan\theta}{1+\chi \tan\theta}}, \quad (1)$$

where θ is the crack deflection angle and χ is the ratio of the mode II to the mode I displacement that occurs during unloading. Llorca [7] used the finite difference technique, in a manner similar to the finite element model of Newman and Armen, to demonstrate the effect of periodic and irregular crack deflection for low ΔK plane strain conditions. It was shown that increasing levels of crack closure occur with increasing crack deflection angle, which are further enhanced by varying deflection angle along a given crack path. As noted earlier, for crack roughness to enhance closure levels, some residual shear offset of the fracture surfaces must exist. The only source of this offset can be plasticity effects at the crack tip. However, these do not appear to be fully addressed in Llorca's work. In particular, there is no refinement of the mesh to accurately account for the expected scale of crack tip plasticity.

Scope and objectives of the present work. The present work is concerned with the finite element modelling of crack closure, arising from the combined effects of crack deflection and prior plastic deformation, in a long fatigue crack in an aerospace aluminium alloy under constant amplitude cyclic loading such that small scale yielding conditions exist at the crack tip. This has been done through an extension of the fatigue crack growth modelling concepts of Newman and Armen [5] to the case of a periodically deflected crack. Continuum plasticity theory has been used with attention being paid to accurate modelling of crack tip plasticity in line with recommendations from the literature[8]. The underlying mechanism leading to the observed RICC has been identified through the isolation of the effects of deflected crack propagation and the effects of plastic deformation at the crack tip. Additionally, a novel approach has been taken to simulate the localisation of strain within the planar slip bands ahead of the crack tip, and the associated influences on shear offsets during crack growth.

The finite element models.

The general purpose finite element code ABAQUS [9] was used to model a standard centre cracked plate (CCP) specimen geometry, as defined by ASTM E647 [10], for width W = 75mm, initial crack length a = 7.6mm, thickness B = 7.5mm, and notch height h = 1mm. Symmetry considerations allowed one half of the specimen to be modelled for deflected crack growth (one quarter for the undeflected crack models). Material properties analogous to a damage tolerant aluminium alloy were chosen. i.e. yield stress σ_0 = 370 MPa, Young's modulus E = 74 GPa, hardening modulus H = 0.07E, Poisson's ratio ν = 0.3. These were implemented in a standard linear kinematic hardening model. Plane strain conditions were assumed. A load of ΔK = 4.6 MPam^{½} at R = 0, corresponding to the near threshold fatigue regime in which RICC processes are prominent was applied. Four different crack geometries were modelled; an undeflected crack, and cracks undergoing periodic deflections of 30°, 45° and 60°.

A procedure for incremental crack propagation was developed along the lines of Newman and Armen's work [5]. Nodes along the crack line were initially connected by two (very short) linear spring elements of cross-section A. The first spring element had no stiffness in compression but was very stiff in tension (>10^4 x E/A). The second spring element was very stiff in compression, but had no stiffness in tension, with the spring stiffness acting normal to the crack face so as to prevent crack face interpenetration without affecting the relative shear displacement of the crack faces. Crack propagation was simulated by removing the tension spring element at the crack tip

node at maximum load. This allowed the crack to grow one element dimension as the original crack tip nodes were no longer constrained in tension.

Slip band simulation. To simulate the presence of slip heterogeneity associated with planar slip bands ahead of a crack tip, the properties of the tension spring elements ahead of the propagating crack tip were modified to restrain the nodes normal to the line of the crack only, i.e. shear displacement of the nodes could then occur. To restrain the nodes in shear, additional rigid-perfectly plastic truss elements were inserted. By controlling the yield stress of these truss elements the effective critical resolved shear stress (CRSS) along the crack propagation direction was varied. To simulate a local strain softening of the material in the slip band, the yield stress of the truss element was set to $\lambda\tau_0$ where λ is a constant specifying the relative strength of the slip band and bulk material (i.e. λ is < 1 for slip band softening) and τ_0 is the bulk CRSS ($= \frac{1}{2}\sigma_0$). It should be noted that in this model the geometry of the slip band is defined by the geometry of the predefined crack path (i.e. secondary slip bands are not included), and the single band that extends ahead of the crack tip at any point is constrained to the distance to the next (pre-determined) deflection point.

Closure assessment. Closure of the crack was determined by monitoring the forces in the compression spring elements behind the tip, in conjunction with the specimen compliance (i.e. load versus displacement) at various locations analogous to the clip/strain gauges used in experimental closure determination, i.e. at the crack mouth, just behind the crack tip, and on the back face of the specimen.

Results and discussion

The effect of periodic crack deflection on K_{cl}/K_{max} can be seen from the plot of the deformed mesh of a 45° deflected crack at $K < K_{cl}$ in Fig. 1. Closure can be seen to have occurred at discrete points near the asperity tips, with the bulk of the crack remaining open, as noted by Walker and Beevers [4]. From Fig. 2, it is evident that the closure levels increase strongly with deflection angle. It appears that quasi-stabilised levels of closure are reached when the crack has propagated through the first two deflections. The closure levels are at a maximum immediately following a deflection, and then drop off steadily as the crack tip moves away from the point of deflection.

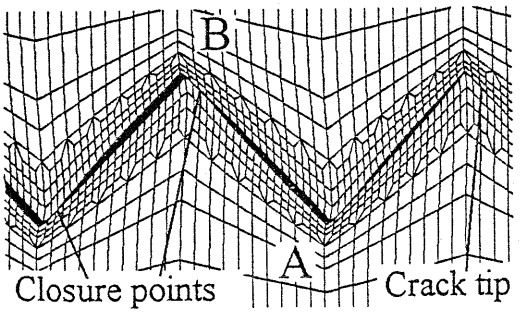

Fig. 1. Crack closure in a 45° deflected crack

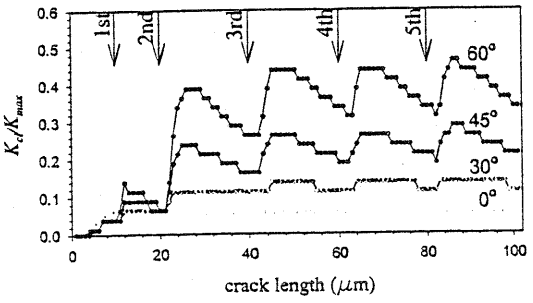

Fig. 2. Variation of closure with crack length and deflection angle. Deflection points marked.

An important observation from these results is the sense of the shear displacements giving rise to asperity contact. In particular it may be seen that the direction of the relative displacements of the upper and lower fracture surfaces at each asperity changes along the crack wake. At point 'A' in Fig. 1 the lower fracture surface is displaced away from the crack tip (in relation to the upper fracture surface), whilst at point 'B' it is displaced towards the crack tip. It may then be seen that the shear displacements giving rise to closure along the crack wake cannot be 'global' displacements of the upper and lower fracture surfaces due to mixed mode behaviour at the active

crack tip. The asperity shear displacements in Fig. 1 can in fact only arise from local residual strains from the crack propagation process. The asperity displacements and contacts observed in the present models are therefore somewhat different to the conventional representation of RICC. The behaviour of the present models may be rationalised as follows: When a simple deflected crack tip is loaded as shown in Fig. 3(a), a permanent plastic shear deformation is produced in the direction/sense shown. On unloading, a degree of reverse plasticity will occur, although a net residual deformation will remain in the direction of the original loading. As such, the crack tip will held in a 'compressive' shear (of opposite sense to the loading shear) by the surrounding elastic material when unloading occurs, exactly analogous to the compressive load generated by crack tip plasticity when a simple mode I crack is unloaded. When turning of the crack occurs, as shown in Fig. 3(c), this residual plastic strain/compressive loading will always promote closure on the forward edge of each asperity tip, as seen in Fig. 1.

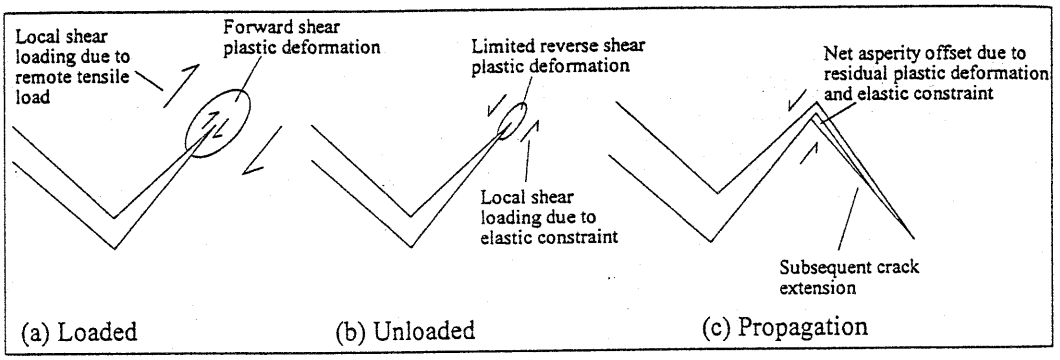

Fig. 3. Crack closure due to residual shear deformation in the crack wake.

To illustrate the above process, various simplified models were investigated. Fig. 4 illustrates the unloaded condition of a deflected crack where the crack path was simply 'cut' without a propagation process, with the crack then being loaded and unloaded once, with the resultant plastic deformation producing a degree of shear offset along the asperities. The shear is of identical direction for all asperities, consistent with deformation at the tip being the only source of shear offset, but is in fact insufficient for any closure to occur due to the associated residual opening displacements. In Fig. 5 the crack has been propagated with loading and unloading only being applied at each crack turning point. For the final crack length shown the crack is simply loaded and unloaded elastically, i.e. no shear offset may be generated by the tip. Closure behaviour is seen to be closely analogous to that in Fig. 1, confirming the role of residual plastic shear displacements

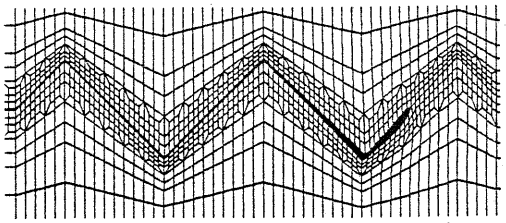

Fig. 4. Residual deformation of a deflected crack loaded and unloaded once.

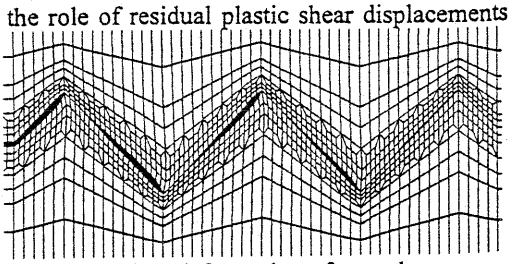

Fig. 5. Residual deformation of a crack loaded and unloaded at each turning point.

along the crack wake in producing closure. It may be seen that the predominant closure process is in fact closely analogous to PICC in mode I loading, although it does rely on crack path roughness to generate the necessary shear displacements. It is important to note that plane stress conditions are not particularly necessary to the asperity contact process shown in Fig. 3 (i.e. as seen in mode I

PICC), as the critical deformations are shear in nature and do not require through-thickness contraction for volume conservation.

The dependence on deflection angle of the closure levels may be compared to the simple analytical model of RICC presented by Suresh and Ritchie [6] for various values of χ, a measure of the fracture surface offset, as shown in Fig. 6 with the finite element results being represented by

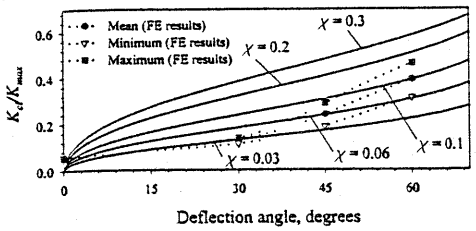

Fig. 6. Comparison of present results to analytical model of Suresh and Ritchie [6].

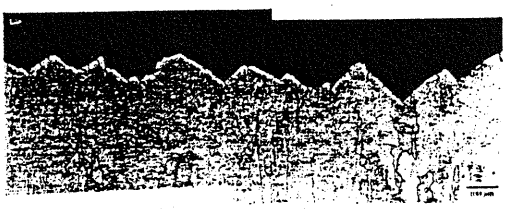

Fig. 7. Deflected crack growth in 8090 Al-Li alloy

the minimum, maximum, and mean quasi-stabilised closure levels. It can be seen that there is no single value of χ which accurately reflects the dependence on the deflection angle of the present results. However, given that the proposed mechanism by which closure is occurring is governed by local shear deformation effects, the value of χ would itself be expected to be dependent on the deflection angle. Values of χ have been evaluated from the finite element results, and are shown in Table 1. The data presented are for the first asperity behind the tip, at which closure occurs first and which can be expected to be the most important asperity in controlling the closure process. It can be seen that the actual values of χ are close to those required to produce comparable closure levels from the Suresh and Ritchie model, and approaching $\chi \sim 0.3$ suggested by Suresh and Ritchie for crack growth in high strength Al alloy plate. In terms of the physical relevance of the current predicted closure levels it is of course difficult to compare the present results to experimental data in the literature given the considerable variability that exists in closure measurement [11], and the relatively idealised crack morphology used here. Al-Li alloys are of some interest in this respect given the strong crystallographic texture levels commonly seen in wrought material and propensity for crystallographic crack growth which may lead to unusually regular crack development e.g. see Fig. 7, corresponding to crack growth in commercial AA8090 plate [12]. Work by Liu et al [12] on TL orientation tests in brass textured plate has shown deflection angles to be very close to 60° (due to the preferred {111} plane orientations), with corresponding closure levels being measured as ~0.7, consistent with similar data in the literature [1]. As such, the present K_{cl} predictions may be seen to be relatively low, although it is important to recognise that: (1) the present models do not include environmental contributions to crack tip irreversibility, (2) there is still a significant degree of crack path irregularity in Fig. 7 (the results of Llorca [6] would imply an enhancement in closure levels with crack path irregularity), (3) the results in Fig. 2 assume a simple homogeneous plastic deformation mode which clearly differs from the intrinsically heterogeneous slip band behaviour giving rise to the observed crack paths. Whilst the first two factors may contribute to the under prediction of closure levels, their effect cannot be explicitly quantified here. In terms of deformation effects however, the influence of a simulated slip band ahead of the crack tip is shown in Fig. 8, for a 60° deflected crack after the onset of closure, with the constant λ set to ½, i.e. τ_0 in the slip band is half that of the bulk material. It can be seen that ahead of the crack tip a significant residual shear offset has developed. The effect that this offset has on the closure levels can be seen by comparison of the predictions of the slip band model to those of the standard models, as shown in Fig. 9. For the 30° deflected crack the effect of the simulated slip band is fairly small, leading to an 18 % increase in

θ, [°]	χ at 1st asperity
30	0.047
45	0.055
60	0.270

Table 1. χ from the present results.

the maximum closure stress. With increasing angle the effect becomes more significant leading to a 40 % increase in closure levels for the 60° deflected crack. In all cases the closure levels return to those of the standard model immediately prior to a deflection. This is due to the active slip band effectively ending at the next deflection point, therefore as the crack approaches the next deflection point the slip band effect is essentially removed by the surrounding constraint. Whilst this represents a quite simple approximation to the presence of a strain softened slip band ahead of a crack tip, it may be seen that there is an increase in closure levels to values which are more consistent with those determined experimentally.

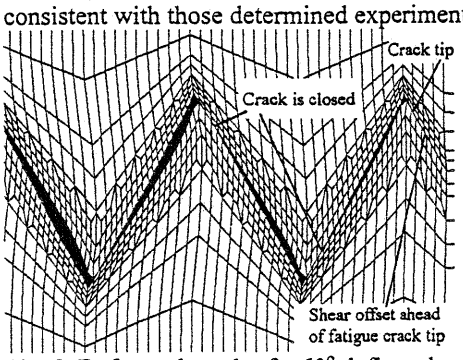

Fig. 8. Deformed mesh of a 60° deflected crack with a slip band.

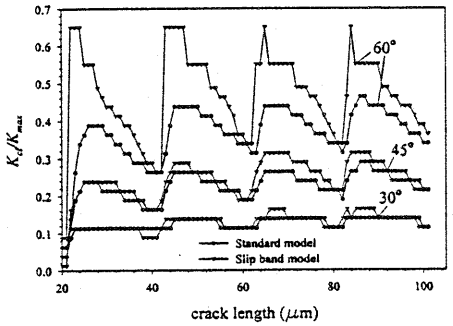

Fig. 9. Effect of slip localisation on the closure level for deflected crack geometries.

Conclusions

(1). Existing finite element techniques have been extended to investigate crack closure arising from crack deflection and plasticity.
(2). Periodic crack deflection has been shown to significantly increase crack closure levels in plane strain, with the effect increasing with deflection angle in reasonable agreement with Suresh and Ritchie's analytical model.
(3). The closure mechanism has been shown to be strongly dependent on the local residual strains arising from the crack propagation process, rather than 'global' shear displacements due to mixed-mode behaviour at the crack tip.
(4). A novel technique for simulating the effect of a planar slip band ahead of a fatigue crack has been implemented. The presence of these bands has been shown to significantly enhance predicted closure levels, consistent with those determined experimentally.

References

[1] K.T. Venkateswara Rao and R.O. Ritchie, Int. Mater. Rev. Vol. 37 (1992) pp.153-185.
[2] W. Elber, Engng. Fract. Mech. Vol. 2 (1970) pp.37-45.
[3] R.O. Ritchie, Mater. Sci. Engng. Vol. A103 (1988) pp.15-28.
[4] N. Walker and C.J. Beevers, Fatigue Engng. Mater. Struct. Vol. 1 (1979) pp.135-148.
[5] J.C. Newman, Jr. and H. Armen, AIAA J. Vol. 13 (1975) pp.1017-1023.
[6] S. Suresh and R.O. Ritchie, Metall. Trans. Vol. 13A (1982) pp.1627-1631.
[7] J. Llorca, Fatigue Fract. Engng. Mater. Struct. Vol. 15 (1992) pp.655-669.
[8] R.C. McClung and H. Sehitoglu, Engng. Fract. Mech. Vol. 33 (1989) pp.237-252.
[9] ABAQUS v5.8, Hibbitt, Karlsson & Sorensen, Inc., Rhode Island, U.S.A., 1998.
[10] E 647 Volume 03.01, 1996 Annual Book of ASTM Standards, American Society for Testing and Materials, Philadelphia, U.S.A., 1996, p. 570.
[11] E.P. Phillips, NASA TM 101601, 1989.
[12] Y. Liu, P.J. Gregson and I. Sinclair, Unpublished research (1998).